Support Information for "Endocytic proteins drive vesicle growth via instability in high membrane tension environment"

TABLE S1: Notations

Notation	Significance
θ^α	Parameters describing the surface
$\mathbf{r}(\theta^\alpha)$	Position vector to an arbitrary point on the surface
$\mathbf{a}_\alpha$	Tangent vectors at any arbitrary point on the surface
$a_{\alpha\beta}$	Components of the metric tensor
$a^{\alpha\beta}$	Components of the dual metric tensor
$e^{\alpha\beta}$	Components of the permutation tensor
$\varepsilon^{\alpha\beta}$	Components of the permutation tensor density
$\mathbf{n}$	Unit normal to the surface at any arbitrary point
$b_{\alpha\beta}$	Components of the curvature tensor
$\tilde{b}^{\alpha\beta}$	Contravariant adjugate of $b_{\alpha\beta}$
Ω	Reference configuration
ω	Current configuration
Ω_a	Domain over which actin force is applied in reference configuration
ω_a	Domain over which actin force is applied in current configuration
W	Strain Energy density in the current configuration
p	Transmembrane Pressure
V	Volume enclosed by the membrane
H	Mean Curvature
K	Gaussian Curvature
$\mathrm{C}(\theta^\alpha)$	Prescribed Spontaneous curvature field
D	Deviatoric Curvature
$D_0(\theta^\alpha)$	Prescribed deviatoric curvature field
E_b	Total free energy of the bilayer
E_f	Work done by actin forces
J	Determinant of the Jacobian
$\lambda(\theta^\alpha)$	Surface tension field
$\boldsymbol{\lambda}$	Direction of alignment of BAR protein
$\boldsymbol{\mu}$	Direction perpendicular to $\boldsymbol{\lambda}$ of BAR in tangent plane
κ_λ	Curvature along direction $\boldsymbol{\lambda}$
κ_μ	Curvature along direction $\boldsymbol{\mu}$
κ_λ^0	Prescribed Spontaneous Curvature along direction $\boldsymbol{\lambda}$
κ_μ^0	Prescribed Spontaneous Curvature along direction $\boldsymbol{\mu}$
k_B	Bending modulus of bare lipid bilayer
k_G	Gaussian modulus of bare lipid bilayer
$\hat{k}_B(\theta^\alpha)$	Bending modulus in the clathrin coated domain.
$\hat{k}_G(\theta^\alpha)$	Gaussian modulus in the clathrin coated domain (assumed equal to k_G).
$\hat{K}_1(\theta^\alpha)$	Modulus associated with mean curvature. ($\hat{k}_B$ in clathrin coated domain and k_B in bare membrane domain).
$\hat{K}_2(\theta^\alpha)$	Modulus associated with deviatoric curvature. (0 in clathrin coated and bare membrane domain)
$\hat{K}_3(\theta^\alpha)$	Gaussian modulus in BAR coated domain (assumed equal to k_G).
λ^α	Contravariant components of $\boldsymbol{\lambda}$
μ^α	Contravariant components of $\boldsymbol{\mu}$

TABLE S1: Notations (continued)

Notation	Significance
$\mathbf{f}$	Force per unit area in the current configuration
$\tilde{\mathbf{f}}$	Force per unit mass (assumed constant from reference to current configuration)
ρ	Mass per unit area in the current configuration
$\mathbf{u}$	Variation given to the position vector
$\mathbf{u}_t$	Variation in the tangential direction
$\mathbf{u}_n$	Variation in the normal direction
a	Determinant of the metric tensor in the current configuration
A	Determinant of the metric tensor in the reference configuration
$\boldsymbol{\tau}$	Unit tangent vector to the boundary of the surface
$\boldsymbol{\nu}$	Unit normal to the boundary of the surface
M	Bending Moment per unit length
F_ν	In-plane normal force per unit length
F_τ	In-plane shear force per unit length
F_n	Transverse shear force per unit length

TABLE S2: Parameters used for simulations

Symbol	Significance	Value	Ref.
k_B	Bending Modulus of the bare lipid bilayer	20 k_BT	[11, 12]
$\hat{k}_B$	Bending modulus of the clathrin coated domain	200 k_BT	[13]
C	Preferred curvature of the clathrin coat	1/50 nm^{-1}	[14]
p	Transmembrane (osmotic) Pressure in Yeast	1000 Pa	[15]
f	Maximum force applied by actin filaments	100 – 200 pN	[16–18]
f_0	Force intensity applied by actin filaments	$< 2\text{x}10^5$ Pa	[16–18]
H_0	Preferred mean curvature of the BAR coat	$0-(1/30)$ nm^{-1}	[19, 20]
D_0	Preferred deviatoric curvature of the BAR coat	$0-(1/30)$ nm^{-1}	[19, 20]
$\hat{K}_1$	Mean curvature bending modulus of the BAR coat	0 - 200 k_BT	[21]
$\hat{K}_2$	Deviatoric curvature modulus of the BAR coat	0 - 200 k_BT	[21]

I. MODEL DESCRIPTION

We model a bilayer as a two-dimensional surface ω with a non-uniform distribution of crescent or banana shaped BAR proteins. The locus of points on ω is tracked by the position vector $\mathbf{r}(\theta^\mu)$ where θ^μ are the surface coordinates. Here and henceforth, Greek indices range over $\{1, 2\}$ and, if repeated, are summed over that range. The basis vectors on the tangent plane at any point are given by $\mathbf{a}_\alpha = \mathbf{r}_{,\alpha}$ where $()_{,\alpha} = \partial()/\partial\theta^\alpha$. This yields the metric $a_{\alpha\beta} = \mathbf{a}_\alpha \cdot \mathbf{a}_\beta$, and the unit surface normal vector $\mathbf{n} = \mathbf{a}_1 \times \mathbf{a}_2 / |\mathbf{a}_1 \times \mathbf{a}_2|$. The local curvature tensor field is given by $\mathbf{b} = b_{\alpha\beta}\mathbf{a}^\alpha \otimes \mathbf{a}^\beta$ where

$$b_{\alpha\beta} = \mathbf{n} \cdot \mathbf{r}_{,\alpha\beta} = -\mathbf{a}_\alpha \cdot \mathbf{n}_{,\beta} \tag{1}$$

are the coefficients of the second fundamental form, $\mathbf{a}^\alpha = a^{\alpha\beta}\mathbf{a}_\beta$ are the contravariant basis vectors, and $(a^{\alpha\beta}) = (a_{\alpha\beta})^{-1}$ is the dual metric [1]. Symmetry restrictions require the strain energy W for an isotropic fluid membrane [2, 3] to depend only on the mean and the Gaussian

curvatures (H,K) where,

$$\begin{aligned} H &= \frac{1}{2}a^{\alpha\beta}b_{\alpha\beta} = (\kappa_\lambda + \kappa_\mu)/2, \\ K &= \frac{1}{2}\varepsilon^{\alpha\beta}\varepsilon^{\theta\psi}b_{\alpha\theta}b_{\beta\psi} = \kappa_\lambda\kappa_\mu - \tau^2. \end{aligned} \tag{2}$$

Here $\{\kappa_\lambda, \kappa_\mu\}$ are the principal curvatures, τ is the twist, and $\varepsilon^{\alpha\beta} = a^{-\frac{1}{2}}e^{\alpha\beta}$ is the permutation tensor density where $e^{\alpha\beta}$ is the permutation tensor. The total free energy of a bilayer that accounts for the areal and volume constraints is given by

$$E_b = \int_\omega (W(H, K; \theta^\alpha) + \lambda(\theta^\alpha))da - pV(\omega), \tag{3}$$

where λ is the surface tension field which is the Lagrange multiplier associated with the local area constraint, p is the transmembrane pressure which is the Lagrange multiplier associated with the volume constraint and V is the enclosed volume.

Clathrin coat: Clathrin coat imparts isotropic spontaneous curvature $C(\theta^\alpha)$ and enhanced flexural stiffness to a bilayer. This results in a modified strain energy $W = \hat{k}_B(\theta^\alpha)(H - C(\theta^\alpha))^2 + \hat{k}_G(\theta^\alpha)K$ in the coated domain. In our model, coat-induced properties $(C, \hat{k}_B, \hat{k}_G)$ can spatially vary, and hence depend on surface coordinates. The specific values of the parameters used in this study are presented in Table S2. Further, we have assumed $\hat{k}_G$ to be the same as k_G.

BAR coat: BAR dimers form a cylindrical coat in contrast to a spherical coat formed by clathrin proteins. As a consequence they generate anisotropic spontaneous curvatures. This breaks the isotropic symmetry present in the above theory and requires the strain energy to depend on a new invariant

$$D = \frac{1}{2}b_{\alpha\beta}(\lambda^\alpha\lambda^\beta - \mu^\alpha\mu^\beta) = (\kappa_\lambda - \kappa_\mu)/2 \tag{4}$$

called the curvature deviator [4–7] . Here $\boldsymbol{\lambda}$ corresponds to the direction of attachment of the BAR dimer and $\boldsymbol{\mu}$ is the direction orthogonal to $\boldsymbol{\lambda}$ in the tangent plane of the surface such that $\{\boldsymbol{\lambda}, \boldsymbol{\mu}, \mathbf{n}\}$ form a local triad (Fig S1). λ^α and μ^α represent the contravariant components of $\boldsymbol{\lambda}$ and $\boldsymbol{\mu}$, respectively (for example, $\lambda^\alpha = \boldsymbol{\lambda} \cdot \mathbf{a}^\alpha$). $\{\kappa_\lambda, \kappa_\mu\}$ represent the curvatures along directions $\boldsymbol{\lambda}$ and $\boldsymbol{\mu}$ respectively. We would like to emphasize that the scalar λ is the surface tension field and the vector $\boldsymbol{\lambda}$ is the direction of attachment of the BAR proteins.

The energy functional in the BAR coated domain takes the form

$$E_b = \int_\omega (W(H, D, K; \theta^\alpha) + \lambda(\theta^\alpha))da - pV(\omega). \tag{5}$$

For our study, we allow the modified strain energy to have a quadratic dependence on H and D, in alignment with the Helfrich energy, and set $\mathrm{W} = \hat{K}_1(\theta^\alpha)(H - C(\theta^\alpha))^2 + \hat{K}_2(\theta^\alpha)(D - D_0(\theta^\alpha))^2 + \hat{K}_3K$. The specific values of these parameters are presented in Table S2. Similar to clathrin coat, we have assumed the Gaussian modulus $\hat{K}_3$ to be the same as k_G.

Force from actin filaments: Let $\mathbf{f}$ be the force per unit area (force intensity) applied by actin filaments on a point on the surface with a position vector $\mathbf{r}$ in the current configuration and $\mathbf{r}_0$ in the reference configuration. The total work done by the applied force over the subdomain on which actin force acts is given by

$$E_f = \int_{\omega_a} \mathbf{f}(\theta^\alpha) \cdot (\mathbf{r} - \mathbf{r}_0)\, da. \tag{6}$$

This results in an augmented free energy

$$E = E_b - E_f. \tag{7}$$

Seamless heterogeneity: The effective membrane properties under the influence of clathrin and BAR proteins and the forces due to actin filaments are specified via a hyperbolic tangent function (tanh) as shown in Fig. S2. This ensures continuity and differentiability of the strain energy density, W, at the interfaces of the protein coated membrane or the actin forcing domain.

A. Variations

We consider a family of surfaces generated by $\mathbf{r}(\theta^\alpha;\epsilon)$. The virtual displacement of the surface is given by $\mathbf{u}(\theta^\alpha) = \frac{\partial}{\partial\epsilon}\mathbf{r}(\theta^\alpha;\epsilon)_{|\epsilon=0} = \dot{\mathbf{r}}$, where the superposed dot refers to the derivative with respect to the parameter ϵ [8]. The variation of the total free energy of the membrane-protein system can be written as

$$\dot{E} = \dot{E}_b - \dot{E}_f \tag{8}$$

where

$$\dot{E}_b = \int_\omega \dot{W} da + \int_\omega (W + \lambda)(\dot{J}/J)\, da - p\dot{V}, \tag{9}$$

$$\dot{E}_f = \int_\omega \mathbf{f} \cdot \mathbf{u}\, da, \tag{10}$$

and $J = \sqrt{a/A}$ is the ratio of the material area after and before the deformation. We follow the procedure outlined in [7–9] to derive the corresponding variational derivatives and the Euler-Lagrange equations. We skip the details and summarize the key intermediate steps and expressions.

Eqs. (2) and Eq. (4) yield the variational derivatives of the three invariants

$$\begin{aligned} 2\dot{H} &= -b^{\alpha\beta}\dot{a}_{\alpha\beta} + a^{\alpha\beta}\dot{b}_{\alpha\beta}, \\ 2\dot{K} &= e^{\alpha\beta}e^{\lambda\mu}\left[\frac{\dot{b}_{\alpha\lambda}b_{\beta\mu}}{a} - \frac{b_{\alpha\lambda}b_{\beta\mu}}{a}\frac{\dot{a}}{a}\right], \end{aligned} \tag{11}$$

and

$$\begin{aligned}\dot{D} &= \frac{1}{2}(\dot{\kappa}_\lambda - \dot{\kappa}_\mu) \\ &= \frac{1}{2}\Big[(\dot{b}_{\alpha\beta}\lambda^\alpha\lambda^\beta + 2b_{\alpha\beta}\dot{\lambda}^\alpha\lambda^\beta) - (\dot{b}_{\alpha\beta}\mu^\alpha\mu^\beta + 2b_{\alpha\beta}\dot{\mu}^\alpha\mu^\beta)\Big].\end{aligned} \tag{12}$$

Using the definitions discussed earlier, we can compute the following variational derivatives of the key geometric quantities

$$\dot{a}_{\alpha\beta} = \mathbf{a}_\alpha \cdot \mathbf{u}_{,\beta} + \mathbf{a}_\beta \cdot \mathbf{u}_{,\alpha}, \tag{13}$$

$$\dot{b}_{\alpha\beta} = \mathbf{n} \cdot \mathbf{u}_{;\alpha\beta}, \tag{14}$$

$$\frac{\dot{a}}{a} = a^{\alpha\beta}\dot{a}_{\alpha\beta}, \tag{15}$$

$$\frac{\dot{J}}{J} = \tfrac{1}{2}a^{\alpha\beta}\dot{a}_{\alpha\beta}, \tag{16}$$

$$\dot{\lambda}^\alpha = a^{\alpha\gamma}(\boldsymbol{\lambda} \cdot \dot{\mathbf{a}}_\gamma) + (\boldsymbol{\lambda} \cdot \mathbf{a}_\gamma)\dot{a}^{\alpha\gamma}, \tag{17}$$

and

$$\dot{\mu}^\alpha = a^{\alpha\gamma}(\boldsymbol{\mu} \cdot \dot{\mathbf{a}}_\gamma) + (\boldsymbol{\mu} \cdot \mathbf{a}_\gamma)\dot{a}^{\alpha\gamma}. \tag{18}$$

Since variation $\mathbf{u}$ can be decomposed into a tangential component $\mathbf{u}_t = u^\eta \mathbf{a}_\eta$, and a normal component $\mathbf{u}_n = u\mathbf{n}$, we derive the equilibrium equations for the two components independently.

1. Tangential Variations

For tangential variations, $\mathbf{u} = u^\lambda \mathbf{a}_\lambda$, which yields

$$\mathbf{u}_{,\alpha} = u^\beta_{;\alpha}\mathbf{a}_\beta + (u^\lambda b_{\lambda\alpha})\mathbf{n} \tag{19}$$

where $()_{;\alpha}$ signifies the covariant derivative. If we substitute it into Eqs. (11)-(18) and carry out simplifications outlined in [7–9], we obtain

$$\dot{a}_{\alpha\beta} = u_{\alpha;\beta} + u_{\beta;\alpha}. \tag{20}$$

$$\dot{b}_{\alpha\beta} = u^\lambda_{;\beta} b_{\lambda\alpha} + u^\lambda_{;\alpha} b_{\beta\lambda} + u^\lambda b_{\lambda\alpha;\beta} \tag{21}$$

$$\frac{\dot{J}}{J} = u^{\alpha}_{;\alpha}. \tag{22}$$

$$\dot{\lambda}^{\alpha} = -\lambda^{\psi} u^{\alpha}_{;\psi}, \quad \text{and} \quad \dot{\mu}^{\alpha} = -\mu^{\psi} u^{\alpha}_{;\psi}. \tag{23}$$

$$\dot{H} = u^{\alpha} H_{,\alpha} \tag{24}$$

$$\dot{K} = u^{\alpha} K_{,\alpha} \tag{25}$$

$$\begin{aligned} \dot{D} = \frac{1}{2}\dot{b}_{\alpha\beta}(\lambda^{\alpha}\lambda^{\beta} - \mu^{\alpha}\mu^{\beta}) + b_{\alpha\beta}[a^{\alpha\gamma}\dot{\mathbf{a}}_{\gamma} \cdot (\lambda^{\beta}\boldsymbol{\lambda} - \mu^{\beta}\boldsymbol{\mu}) \\ + \dot{a}^{\alpha\gamma}\mathbf{a}_{\gamma} \cdot (\lambda^{\beta}\boldsymbol{\lambda} - \mu^{\beta}\boldsymbol{\mu})]. \end{aligned} \tag{26}$$

Furthermore,

$$\begin{aligned} &\dot{W} = W_H \dot{H} + W_D \dot{D} + W_K \dot{K}, \quad \text{and} \\ &W_{,\eta} = W_H H_{,\eta} + W_D D_{,\eta} + W_K K_{,\eta} + \partial W/\partial\theta^{\eta}. \end{aligned} \tag{27}$$

Using the above obtained relations, we deduce the in-plane equilibrium equation (for $\dot{E} = 0$)

$$\lambda_{,\eta} = -\partial W/\partial\theta^{\eta} - W_D(b_{\alpha\beta}(\lambda^{\alpha}\lambda^{\beta})_{;\eta}) - \mathbf{f} \cdot \mathbf{a}_{\eta}. \tag{28}$$

This equation regulates the spatial variation of the surface tension field. It is operative when the membrane has heterogeneous properties and is trivially satisfied for homogeneous membranes. In the clathrin coated and bare lipid membrane domains, dependence of W on D is suppressed.

2. Normal Variations

For normal variations, $\mathbf{u} = u(\theta^{\alpha})\mathbf{n}$. This yields

$$\mathbf{u}_{,\alpha} = u_{,\alpha}\mathbf{n} - u b^{\beta}_{\alpha}\mathbf{a}_{\beta}. \tag{29}$$

Again, substituting Eq. (29) into Eqs. (11)-(18) and carrying out simplifications outlined in [7–9] furnish

$$\dot{a}_{\alpha\beta} = -2u b_{\alpha\beta}, \tag{30}$$

$$\dot{b}_{\alpha\beta} = u_{;\alpha\beta} - u b_{\alpha\lambda} b^{\lambda}_{\beta}, \tag{31}$$

$$\dot{J}/J = -2Hu, \tag{32}$$

$$\dot{\lambda^{\alpha}} = u b^{\gamma}_{\psi} a^{\alpha\psi}\lambda_{\gamma}, \qquad \dot{\mu^{\alpha}} = u b^{\gamma}_{\psi} a^{\alpha\psi}\mu_{\gamma}, \tag{33}$$

$$2\dot{H} = \Delta u + u(4H^2 - 2K), \tag{34}$$

$$\dot{K} = 2KHu + \tilde{b}^{\alpha\beta}u_{;\alpha\beta}, \tag{35}$$

$$\dot{D} = (u_{;\alpha\beta} + ub_{\alpha\gamma}b^{\gamma}_{\beta})(\lambda^{\alpha}\lambda^{\beta} - \mu^{\alpha}\mu^{\beta})/2, \tag{36}$$

where $\Delta = ()_{;\alpha\beta}a^{\alpha\beta}$ denotes the surface Laplacian.

Also,

$$\dot{V} = \int_{\omega} \mathbf{u}\cdot\mathbf{n}\, da \; = \int_{\omega} u\, da \tag{37}$$

Using the above obtained variations, we obtain the song Euler-Lagrange question, called the *shape equation* that governs the geometry of the membrane

$$\begin{aligned}&\frac{1}{2}[W_D(\lambda^{\alpha}\lambda^{\beta} - \mu^{\alpha}\mu^{\beta})]_{;\beta\alpha} + \frac{1}{2}W_D(\lambda^{\alpha}\lambda^{\beta} - \mu^{\alpha}\mu^{\beta})b_{\alpha\gamma}b^{\gamma}_{\beta} + \Delta(\frac{1}{2}W_H) + (W_K)_{;\beta\alpha}\tilde{b}^{\beta\alpha}\\ &+ W_H(2H^2 - K) + 2H(KW_K - W) - 2H\lambda = p + \mathbf{f}\cdot\mathbf{n}.\end{aligned} \tag{38}$$

As for the equilibrium equation in the tangent plane, we suppress the dependence of W on D in the clathrin coated and bare lipid membrane domains.

3. Boundary Forces and Moment

In the presence of boundaries, the tangential and normal variations yield additional terms that define the stresses and moments at the boundary [7, 10]. For any arbitrary boundary $\partial\omega$ on the surface, a unit tangent vector $\boldsymbol{\tau}$ (shown in Fig. S3) can be obtained by taking the derivative of the position vector with respect to the arc length that parameterizes the boundary. Thus,

$$\boldsymbol{\tau} = \frac{d\mathbf{r}(\theta^{\alpha}(s))}{ds} \tag{39}$$

and the unit normal to the boundary, in the tangent plane of the surface, can then be defined by the vector $\boldsymbol{\nu} = \boldsymbol{\tau}\times\mathbf{n}$.

Following the procedure outlined in [7, 10], we arrive at the following boundary terms

$$\begin{aligned}\dot{E}_B = &\int_{\partial\omega}(F_{\nu}\boldsymbol{\nu} + F_{\tau}\boldsymbol{\tau} + F_n\mathbf{n})\cdot\mathbf{u}ds - \int_{\partial\omega} M\boldsymbol{\tau}\cdot\boldsymbol{\omega}ds\\ &+ \sum_i \mathbf{f}_i\cdot\mathbf{u}_i\end{aligned} \tag{40}$$

where

$$\begin{aligned}
M &= \frac{1}{2}W_H + \kappa_\tau W_K + W_D\lambda^\alpha\lambda^\beta\nu_\beta\nu_\alpha - \frac{1}{2}W_D,\\
F_\nu &= W + \lambda - \kappa_\nu M,\\
F_\tau &= -\tau M,\\
F_n &= (\tau W_K)' - \frac{1}{2}(W_H)_{,\nu} - (W_K)_{,\beta}\tilde{b}^{\alpha\beta}\nu_\alpha,\\
&\quad + \frac{1}{2}(W_D)_{,\nu} - (W_D\lambda^\alpha\lambda^\beta)_{;\beta}\nu_\alpha - (W_D\lambda^\alpha\lambda^\beta\nu_\beta\tau_\alpha)',\\
\mathbf{f}_i &= (W_K[\tau] + W_D[\lambda^\alpha\lambda^\beta\nu_\beta\tau_\alpha])_i\mathbf{n}.
\end{aligned} \tag{41}$$

Square brackets indicate forward jumps in values within the brackets at the corners of a boundary when there is a jump in $\boldsymbol{\tau}$ and $()' = \frac{d()}{ds}$. Above, M is the bending moment per unit length, F_ν is the in-plane normal force per unit length, F_τ is the in-plane shear force per unit length, F_n is the transverse shear force per unit length and $\mathbf{f}_i$ is the force applied at i th corner of $\partial\omega$.

B. Axisymmetric Deformations

We assume that the membrane invaginations possess axisymmetry. We simplify the equilibrium equations (28) and (38) for axisymmetric surfaces parameterized by meridional arc length s and azimuthal angle θ. Since the Gaussian modulus is assumed to be uniform in all the domains (bare membrane, clathrin coat and BAR coat) and the membrane is planar at the boundary of the simulated domain, we can use the Gauss-Bonnet theorem to suppress the dependence of the strain energy density (W) on the Gaussian curvature (K). For such a surface,

$$\mathbf{r}(s,\theta) = r(s)\mathbf{e}_r(\theta) + z(s)\mathbf{k} \tag{42}$$

where $r(s)$ is the radius from axis of revolution, $z(s)$ is the elevation from a base plane and $(\mathbf{e}_r, \mathbf{e}_\theta, \mathbf{k})$ form the coordinate basis. Since $(r')^2 + (z')^2 = 1$, we can define an angle ψ such that

$$r'(s) = \cos\psi \quad \text{and} \quad z'(s) = \sin\psi. \tag{43}$$

As mentioned above, $()' = \partial()/\partial s$. With $\theta^1 = s$ and $\theta^2 = \theta$, we can easily show that

$$\begin{aligned}
&\mathbf{a}_1 = r'\mathbf{e}_r + z'\mathbf{k}, \quad \mathbf{a}_2 = r\mathbf{e}_\theta, \quad \text{and}\\
&\mathbf{n} = -\sin(\psi)\mathbf{e}_r + \cos(\psi)\mathbf{k}.
\end{aligned} \tag{44}$$

Using Eq. (44) and its derivatives, we can show that the metric $(a_{\alpha\beta}) = diag(1, r^2)$, the dual metric $(a^{\alpha\beta}) = diag(1, \frac{1}{r^2})$, and the covariant components of the curvature tensor $(b_{\alpha\beta}) =$

$diag(\psi', r\sin\psi)$. Together they furnish the two invariants

$$\begin{aligned} 2H &= \frac{\sin\psi}{r} + \psi', \quad \text{and} \\ K &= H^2 - (H - (\sin\psi)/r)^2. \end{aligned} \tag{45}$$

For BAR coated domain, we consider a continuous distribution of proteins on the surface with crescent shaped dimers aligned in the circumferential direction. Thus,

$$\boldsymbol{\lambda} = -\mathbf{e}_\theta, \quad \boldsymbol{\mu} = \cos\psi\mathbf{e}_r + \sin\psi\mathbf{k}, \tag{46}$$

and the normal curvatures in the above two directions are $\kappa_\lambda = (\sin\psi)/r$ and $\kappa_\mu = \psi'$, respectively. The curvature deviator is thus given by $D = [(\sin\psi)/r - \psi']/2$. For this choice of $\boldsymbol{\lambda}$ and $\boldsymbol{\mu}$, the shape equation (38) for an axisymmetric geometry reduces to

$$p + \mathbf{f}\cdot\mathbf{n} = \frac{L'}{r} + W_H(2H^2 - K) - 2H(W + \lambda - W_D D) + \frac{((W_D)'\cos\psi)}{r} \tag{47}$$

where

$$L/r = \frac{1}{2}[(W_H)' - (W_D)']. \tag{48}$$

The equilibrium equation in the tangent plane (28) takes the form

$$\lambda' = -W' - \mathbf{f}\cdot\mathbf{a}_1. \tag{49}$$

The above equations remain valid for the uncoated and the clathrin coated membranes by suppressing dependence of strain energy density on the deviatoric curvature D. In order to maintain a control over the domains over which clathrin, actin and BAR proteins interact with the membrane, we transform the independent variable from arclength s to area a with the help of the relation $da/ds = 2\pi r$.

For an axisymmetric case, we can express the strain energy density of the BAR coated domain in terms of curvatures along principal directions $\{\kappa_\lambda, \kappa_\mu\}$

$$W = \hat{k}_1(\kappa_\lambda - \kappa_\lambda^0)^2 + \hat{k}_2(\kappa_\mu - \kappa_\mu^0)^2 + 2\hat{k}_{12}(\kappa_\lambda - \kappa_\lambda^0)(\kappa_\mu - \kappa_\mu^0). \tag{50}$$

The bending moduli in the $\{H, D\}$ and the $\{\kappa_\lambda, \kappa_\mu\}$ framework are related by the following expressions $\hat{k}_1 = \hat{k}_2 = (\hat{K}_1 + \hat{K}_2)$ and $\hat{k}_{12} = (\hat{K}_1 - \hat{K}_2)$.

In addition, we non-dimensionalize the system of equations and define

$$\begin{aligned} &\bar{r} = r/R_0,\ \bar{z} = z/R_0,\ \bar{a} = a/2\pi{R_0}^2,\ \bar{\kappa}_\lambda = R_0\kappa_\lambda,\ \bar{W} = W{R_0}^2/k_0, \\ &\bar{\kappa}_\mu = R_0\kappa_\mu,\ \bar{H} = R_0 H,\ \bar{D} = R_0 D,\ \bar{K} = {R_0}^2 K,\ \bar{\lambda} = \lambda{R_0}^2/k_0, \\ &\bar{L} = R_0 L/k_0,\ \bar{k}_1 = \hat{k}_1/k_0,\ \bar{k}_2 = \hat{k}_2/k_0,\ \bar{p} = p{R_0}^3/k_0,\ \bar{\mathbf{f}} = ({R_0}^3/k_0)\mathbf{f}. \end{aligned} \tag{51}$$

where $R_0 = 25\,nm$ is the normalizing radius of curvature and $k_0 = 20k_BT$ is the normalizing bending modulus.

In terms of these normalized parameters and the partial derivative with respect to a, $\mathring{()} = \partial()/\partial\bar{a}$, the system of equations can be written as

$$\mathring{\bar{r}} = \cos\psi/\bar{r}, \quad \mathring{\bar{z}} = \sin\psi/\bar{r}, \tag{52}$$

$$\mathring{\psi} = \bar{\kappa}_\lambda/\bar{r}, \tag{53}$$

$$\bar{L}/\bar{r}^2 = \frac{1}{2}(\mathring{\bar{W}}_H - \mathring{\bar{W}}_D), \tag{54}$$

$$\mathring{\bar{L}} = \bar{p} + \bar{\mathbf{f}}\cdot\mathbf{n} - \bar{W}_H(2\bar{H}^2 - \bar{K}) + 2\bar{H}(\bar{W} + \bar{\lambda} - \bar{W}_D\bar{D}) - \mathring{\bar{W}}_D\cos\psi, \quad \text{and} \tag{55}$$

$$\mathring{\bar{\lambda}} = -\mathring{\bar{W}} - \bar{\mathbf{f}}\cdot\mathbf{a}_1. \tag{56}$$

In terms of the normalized principal curvatures, Eqs. (54)-(56) can be expressed as

$$\mathring{\bar{L}} = \Big(\bar{p} + \bar{\mathbf{f}}\cdot\mathbf{n} + (\bar{\kappa}_\lambda + \bar{\kappa}_\mu)(W + \bar{\lambda}) - 2\bar{\kappa}_\lambda^2[\bar{k}_1(\bar{\kappa}_\lambda - \bar{\kappa}_\lambda^0) + \bar{k}_{12}(\bar{\kappa}_\mu - \bar{\kappa}_\mu^0)] - 2\bar{\kappa}_\mu^2[\bar{k}_{12}(\bar{\kappa}_\lambda - \bar{\kappa}_\lambda^0) + \bar{k}_2(\bar{\kappa}_\mu - \bar{\kappa}_\mu^0)]\Big) - \mathring{W}_D\cos\psi, \tag{57}$$

$$\mathring{\bar{\kappa}}_\lambda = \frac{(\cos\psi)\bar{\kappa}_\mu}{\bar{r}^2} - \frac{(\sin\psi\cos\psi)}{\bar{r}^3}, \tag{58}$$

$$\begin{aligned}\mathring{\bar{\lambda}} = -\Big(&\mathring{\bar{k}}_1(\bar{\kappa}_\lambda - \bar{\kappa}_\lambda^0)^2 - 2\bar{k}_1(\bar{\kappa}_\lambda - \bar{\kappa}_\lambda^0)\mathring{\bar{\kappa}}_\lambda^0 + \mathring{\bar{k}}_2(\bar{\kappa}_\mu - \bar{\kappa}_\mu^0)^2 - 2\bar{k}_2(\bar{\kappa}_\mu - \bar{\kappa}_\mu^0)\mathring{\bar{\kappa}}_\mu^0 \\ &+ 2\mathring{\bar{k}}_{12}(\bar{\kappa}_\lambda - \bar{\kappa}_\lambda^0)(\bar{\kappa}_\mu - \bar{\kappa}_\mu^0) - 2\bar{k}_{12}(\bar{\kappa}_\mu - \bar{\kappa}_\mu^0)\mathring{\bar{\kappa}}_\lambda^0 - 2\bar{k}_{12}(\bar{\kappa}_\lambda - \bar{\kappa}_\lambda^0)\mathring{\bar{\kappa}}_\mu^0\Big).\end{aligned} \tag{59}$$

Above,

$$\mathring{W}_D = (2\mathring{\bar{k}}_1 - 2\mathring{\bar{k}}_{12})(\bar{\kappa}_\lambda - \bar{\kappa}_\lambda^0) + (2\bar{k}_1 - 2\bar{k}_{12})(\mathring{\bar{\kappa}}_\lambda - \mathring{\bar{\kappa}}_\lambda^0) + (2\mathring{\bar{k}}_{12} - 2\mathring{\bar{k}}_2)(\bar{\kappa}_\mu - \bar{\kappa}_\mu^0) + (2\bar{k}_{12} - 2\bar{k}_2)(\mathring{\bar{\kappa}}_\mu - \mathring{\bar{\kappa}}_\mu^0), \tag{60}$$

and

$$\mathring{\bar{\kappa}}_\mu = \frac{\bar{L}}{2\bar{k}_2\bar{r}^2} + \mathring{\bar{\kappa}}_\mu^0 - \frac{\mathring{\bar{k}}_2}{k_2}(\bar{\kappa}_\mu - \bar{\kappa}_\mu^0) - \frac{\bar{k}_{12}}{k_2}(\mathring{\bar{\kappa}}_\lambda - \mathring{\bar{\kappa}}_\lambda^0) - \frac{\mathring{\bar{k}}_{12}}{k_2}(\bar{\kappa}_\lambda - \bar{\kappa}_\lambda^0). \tag{61}$$

The expressions for the boundary forces and moments reduce to:

$$\begin{aligned}
&F_\tau = -\tau M = 0,\\
&\bar{M} = 2\bar{k}_2(\bar{\kappa}_\mu - \bar{\kappa}^0_\mu) + 2\bar{k}_{12}(\bar{\kappa}_\lambda - \bar{\kappa}^0_\lambda),\\
&F_\nu = W + \lambda - \bar{\kappa}_\mu(2\bar{k}_2(\bar{\kappa}_\mu - \kappa^0_\mu) + 2\bar{k}_{12}(\bar{\kappa}_\lambda - \bar{\kappa}^0_\lambda)),\\
&\bar{F}_\nu = \bar{k}_1(\bar{\kappa}_\lambda - \bar{\kappa}^0_\lambda)^2 + \bar{k}_2(\bar{\kappa}_\mu - \bar{\kappa}^0_\mu)^2 + 2\bar{k}_{12}(\bar{\kappa}_\lambda - \bar{\kappa}^0_\lambda)(\bar{\kappa}_\mu - \bar{\kappa}^0_\mu) + \bar{\lambda} - \bar{\kappa}_\mu(2\bar{k}_2(\bar{\kappa}_\mu - \bar{\kappa}^0_\mu)\\
&\qquad + 2\bar{k}_{12}(\bar{\kappa}_\lambda - \bar{\kappa}^0_\lambda)),\\
&\bar{F}_n = -\bar{L}/\bar{r}.
\end{aligned} \tag{62}$$

Boundary Conditions:

The system of equations to be solved comprises of six simultaneous ODE's (52), (53), (57), (58), and (59). We prescribe the following six boundary conditions at the two ends of the simulation domain as shown in Fig. S4.

i) For the near end at $\bar{a} = 0$

$$\bar{r} = 0, \quad \psi = 0 \quad \text{and} \quad \bar{L} = 0 \,(\text{due to reflection symmetry about z axis}) \tag{63}$$

ii) For the far end at $\bar{a} = \bar{a}_0$

$$\bar{z} = 0, \quad \psi = 0 \quad \text{and} \quad \bar{\lambda} = \bar{\lambda}_0 \,(\text{prescribed far end tension}) \tag{64}$$

The ODE's along with the boundary conditions are solved in Matlab using 'bvp4c solver'.

[1] Kreyszig E (1959). Differential Geometry *University of Toronto Press.*

[2] Steigmann DJ (1999). Fluid films with curvature elasticity. *Arch. Rational Mech. Anal.* 150, 127-152.

[3] Jenkins JT (1977). The equations of mechanical equilibrium of a model membrane. *SIAM Journal on Applied Mathematics* 32(4), 755-764.

[4] Iglic VK, Remskar M, Vidmar G, Fosnaric M, Iglic A (2002). Deviatoric elasticity as a possible physi- cal mechanism explaining collapse of inorganic micro and nanotubes. *Physics Letters A* 296, 151-155.

[5] Iglic VK, Heinrich V, Svetina S, Zeks V (1999). Free energy of closed membrane with anisotropic inclusions. *Eur. Phys. J. B* 10, 5-8.

[6] Fosnaric M et. al (2005). The influence of anisotropic membrane inclusions on curvature elastic properties of lipid membranes. *Chem Inf. Model* 45, 1652-1661.

[7] Walani N, Torres J, Agrawal A (2014). Anisotropic spontaneous curvatures in lipid membranes. *Physical Review E* 89(6), 062715.

[8] Steigmann DJ, Baesu E, Rudd RE, Belak J, McElfresh M (2003). On the variational theory of cell-membrane equilibria. *Interfaces and Free Boundaries* 5, 357-366.

[9] Agrawal A, Steigmann DJ (2009). Modeling protein-mediated morphology in biomembranes. *Biomechanics and modeling in mechanobiology* 8(5), 371-379.

[10] Agrawal A, Steigmann DJ (2009). Boundary-value problems in the theory of fluid films with curvature elasticity *Continuum Mechanics and Thermodynamics*, 21, 57-82.

[11] Duwe HP, Kaes J, Sackmann E (1990). Bending elastic moduli of lipid bilayers: modulation by solutes. *Journal de Physique* 51(10), 945-961.

[12] Faucon JF et. al (1989). Bending elasticity and thermal fluctuations of lipid membranes. Theoretical and experimental requirements. *Journal de Physique* 50(17), 2389-2414.

[13] Jin AJ, Prasad K, Smith PD, Lafer EM, Nossal R (2006). Measuring the elasticity of clathrin-coated vesicles via atomic force microscopy. *Biophysical journal* 90 (9), 3333-3344.

[14] Bonifacino JS, Schwartz JL (2003). Coat proteins: shaping membrane transport. *Nature Reviews Molecular Cell Biology* 4 (5), 409-414.

[15] Gustin MC, Zhou XL, Martinac B, Kung C (1988). A Mechanosensitive Ion Channel in the Yeast Plasma Membrane. *Science* New Series, Vol. 242 (4879), 762-765.
[16] Finer JT, Simmons RM, Spudich JA (1994). Single myosin molecule mechanics: piconewton forces and nanometre steps. *Nature* 368 (6467), 113-119.
[17] Footer MJ, Kerssemakers JWJ, Theriot JA, Dogterom M (2007). Direct measurement of force generation by actin filament polymerization using an optical trap. *Proceedings of the National Academy of Sciences* 104(7), 2181-2186.
[18] Kovar DR, Pollard TD (2004). Insertional assembly of actin filament barbed ends in association with formins produces piconewton forces. *Proceedings of the National Academy of Sciences of the United States of America* 101(41), 14725-14730.
[19] Gallop JL et. al (2006). Mechanism of endophilin N-BAR domain mediated membrane curvature. *The EMBO journal* 25(12), 2898-2910.
[20] Yin Y, Arkhipov A, Schulten K (2009). Simulations of membrane tubulation by lattices of amphiphysin N-BAR domains. *Structure* 17(6), 882-892.
[21] Ayton GS, Blood PD, Voth GA (2007). Membrane remodeling from N-BAR domain interactions: insights from multi-scale simulation. *Biophysical journal* 92(10), 3595-3602.
[22] Kukulski W, Schorb M, Kaksonen M, Briggs JAG (2012). Plasma membrane reshaping during endocytosis is revealed by time-resolved electron tomography. *Cell* 150(3), 508-520.

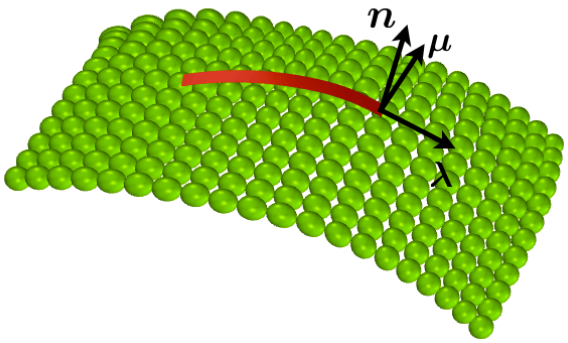

FIG. S1: A BAR protein attached to the surface of a bilayer. $\boldsymbol{\lambda}$ corresponds to the direction of attachment of the BAR dimer, $\boldsymbol{\mu}$ is the direction orthogonal to $\boldsymbol{\lambda}$ in the tangent plane of the surface and $\mathbf{n}$ is the surface normal. Republished figure from ref. [7], Copyright 2014 by the American Physical Society; dx.doi.org/10.1103/PhysRevE.89.062715.

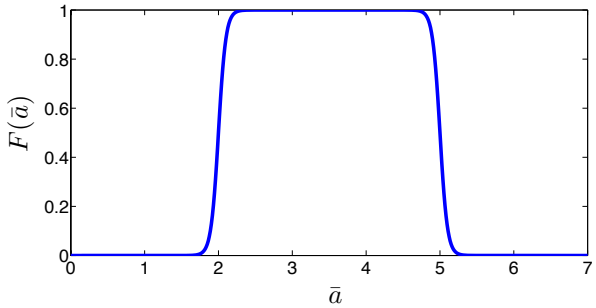

FIG. S2: Function used to prescribe curvature and force fields generated by clathrin, actin and BAR proteins. F($\bar{a}$)= tanh [10($\bar{a} - \bar{a}_1$)] - tanh [10*($\bar{a} - \bar{a}_2$)] with $\bar{a}_1 = 2$, $\bar{a}_2 = 5$. Here, $\bar{a} = \bar{a}_1$ to $\bar{a} = \bar{a}_2$ represents the area over which the the fields are prescribed.

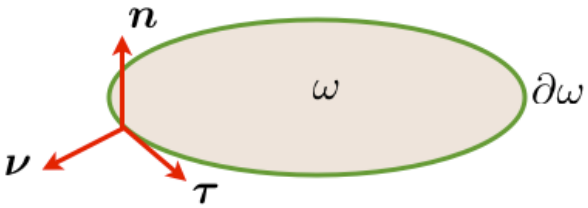

FIG. S3: The three orthonormal vectors on a smooth boundary $\partial\omega$.

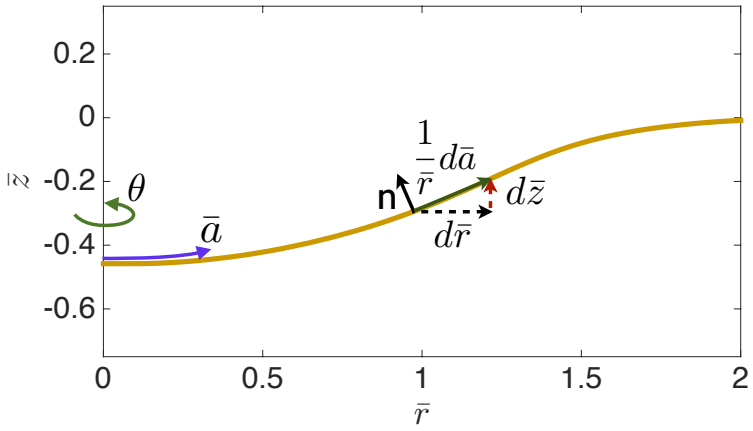

FIG. S4: Simulation domain where the boundary conditions are prescribed at the end points ($\bar{a} = 0$, $\bar{a} = \bar{a}_0$). Here **n** is the vector normal to the surface. Parametrization of the surface is done in terms of area ($\bar{a}$) rather than arc length to control the area over which clathrin and BAR proteins attach to the membrane and actin filaments apply force on the membrane. The direction of increasing area is represented with a purple arrow while the direction of increasing azimuthal angle (θ) is represented with a green curved arrow.

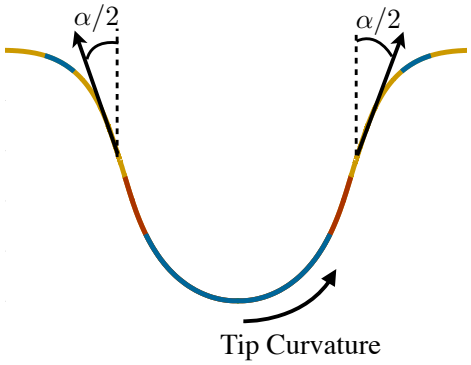

FIG. S5: Angle between the membranes is the minimum angle (α) between membranes in the tubular domain. For a flat configuration this angle is 180^0 where as for the neck it is 0. The tip curvature signifies the radius of curvature at the tip of the vesicle in the plane of the paper. These definitions are obtained from [22].

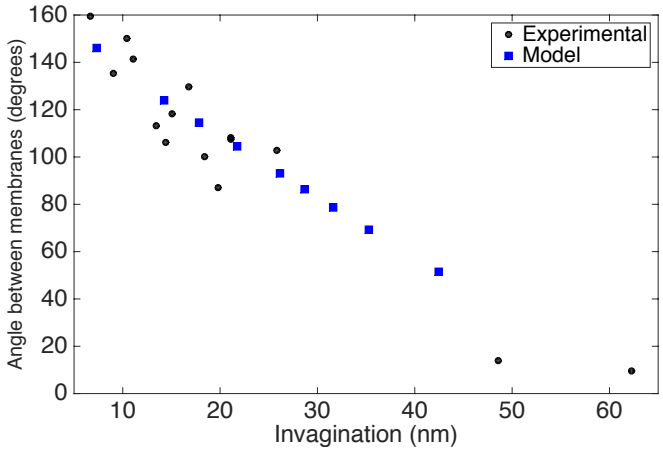

FIG. S6: Variation of angle between the membranes (see Fig. S5) with invagination in the Rvs 167 mutant case. As the vesicle becomes more cylindrical or tubular, the angle between the membranes decreases and eventually, goes to zero. Computed data points in solid blue squares match well with the experimental data in solid black circles. Republished with permission from Elsevier; www.sciencedirect.com/science/journal/00928674.

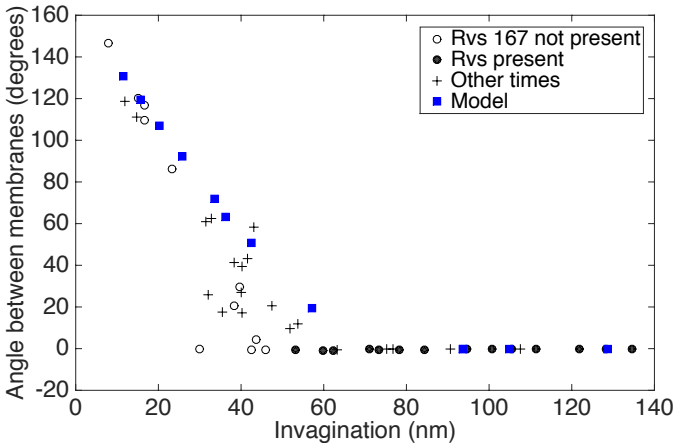

FIG. S7: Variation of angle between the membranes (see Fig. S5) with invagination in the wild type case. As the vesicle becomes more cylindrical or tubular, the angle between the membranes decreases and eventually, goes to zero. Computed data points in solid blue squares match well with the experimental data in solid black circles. Republished with permission from Elsevier; www.sciencedirect.com/science/journal/00928674.

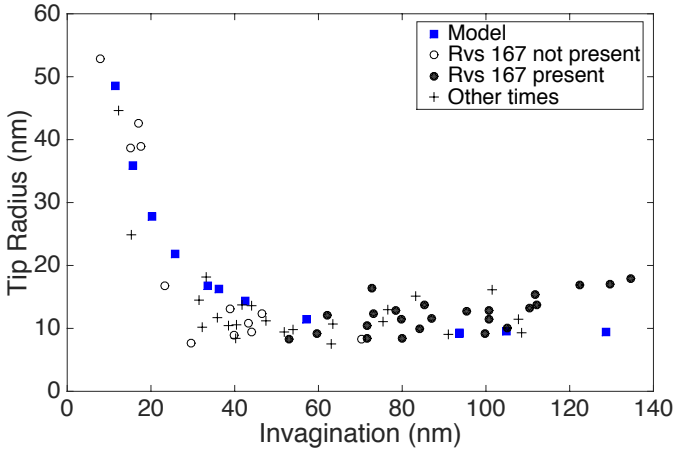

FIG. S8: Variation of radius of curvature at the vesicle tip (see Fig. S5) with invagination. The radius of curvature asymptotically decreases to 10 nm with increasing invagination. Computed data points in solid blue squares match well with the experimental data in black circles. Republished with permission from Elsevier; www.sciencedirect.com/science/journal/00928674.

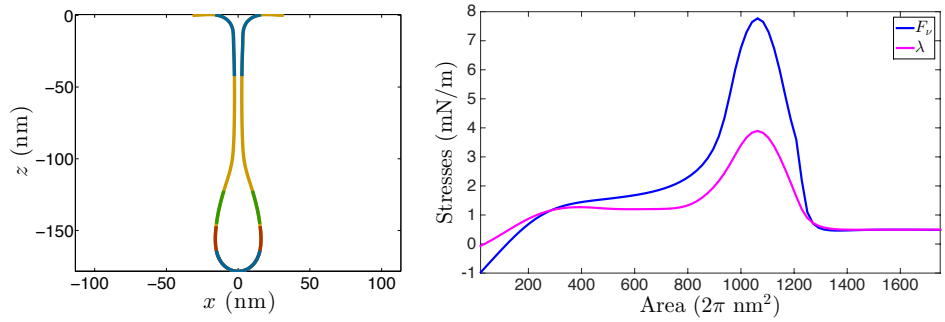

(a) (b)

FIG. S9: Scission stage for BAR-driven invagination. (a) Vesicle shape, and (b) Membrane stresses. Total in-plane stress F_ν crosses the rupture stress of 7.5 mN/m.

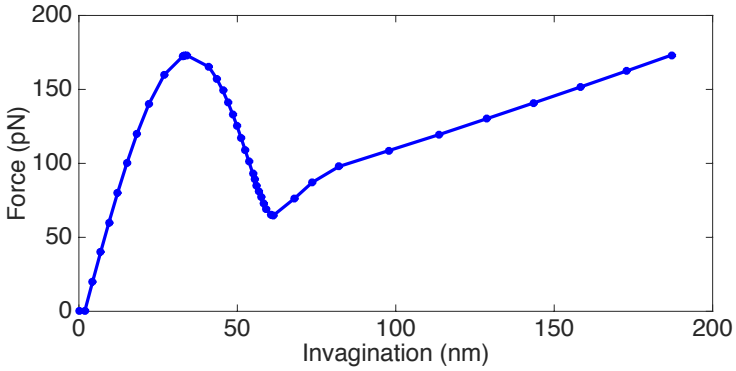

FIG. S10: Actin driven force-deflection response in the absence of clathrin coat. The curve exhibits a snap-through instability as observed in the presence of clathrin. Resting tension in the membrane is 0.5 mN/m.

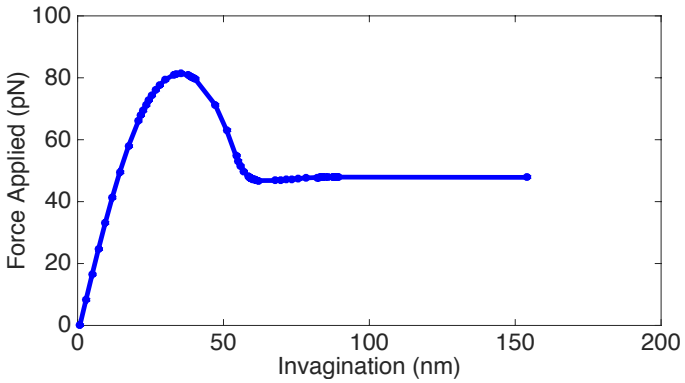

FIG. S11: Force-deflection response in the absence of clathrin coat and counter forces in the planar membrane adjacent to the vesicle site. Unlike the force-deflection curve in Fig. S10, the curve exhibits a horizontal third branch. Resting tension in the membrane is 0.5 mN/m.

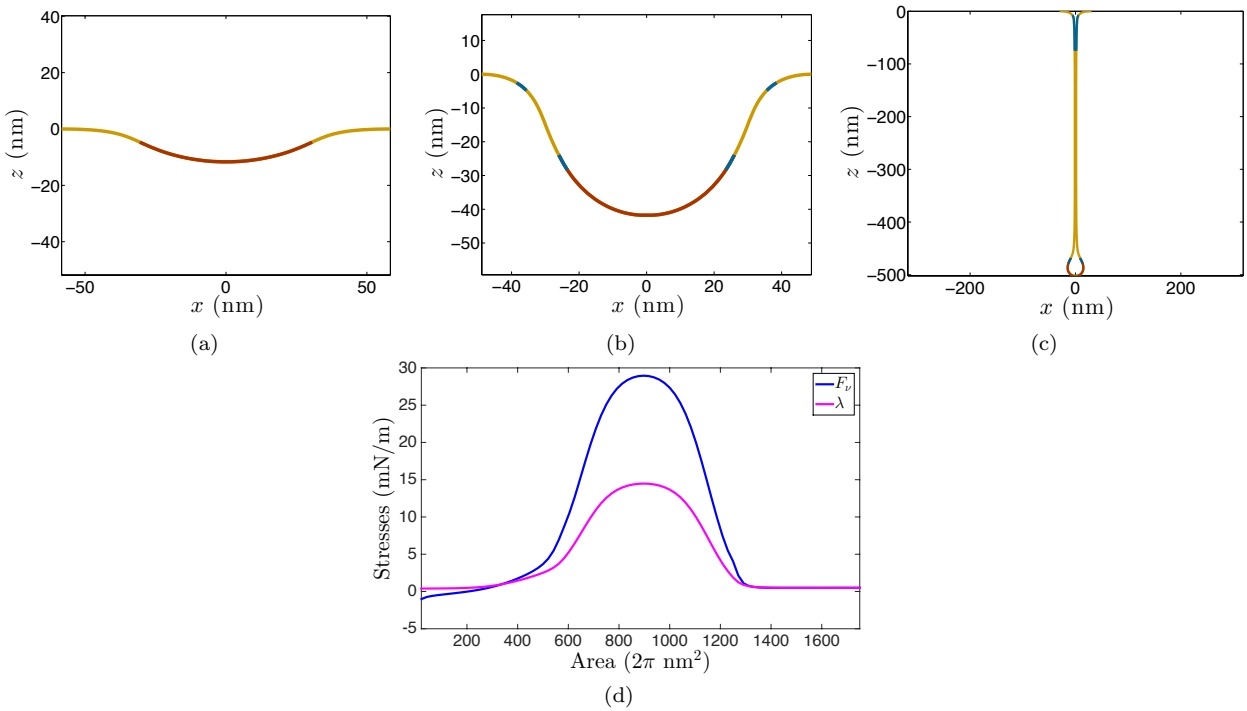

FIG. S12: Actin-driven vesicle growth for actin loading II. (a)-(c) Vesicle shapes at different stages. (d) Stress profile for the shape after snap-through instability shown in (c). The behavior is almost similar to loading I.

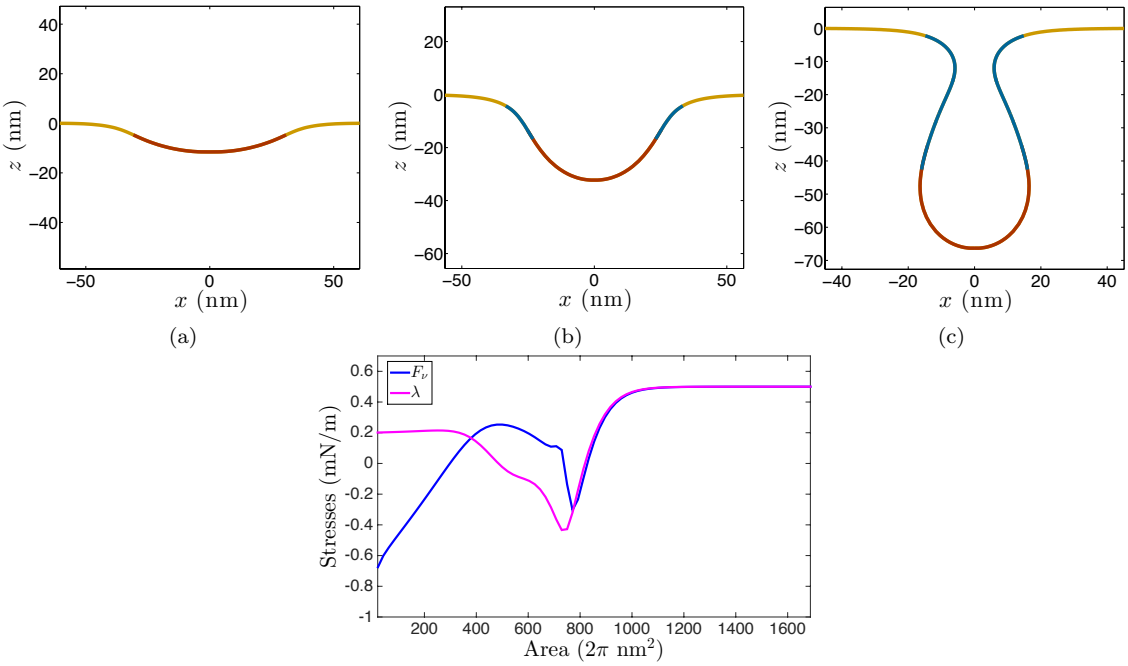

FIG. S13: Actin-driven vesicle growth for actin loading III. (a)-(c) Vesicle shapes at different stages. (d) Stress profile for the shape after snap-through instability shown in (c). In contrast to the other two loadings, the peak stress in the tubular domain in (c) reaches only 0.25 mN/m.